

# Numerical study and optimization of a diffraction grating for surface plasmon excitation

Gaëtan Lévêque and Olivier J. F. Martin

Swiss Federal Institute of Technology Lausanne, Nanophotonics and Metrology Laboratory  
EPFL-STI-NAM, Station 11, CH-1015 Lausanne, Switzerland

## ABSTRACT

The numerical study of plasmonic optical objects is of great importance in the context of massive integration of light processing devices on a very small surface. A wide range of nanoobjects are currently under study in the scientific community like stripe waveguides, Bragg's mirrors, resonators, couplers or filters. One important step is the efficient coupling of a macroscopic external field into a nanodevice, that is the injection of light into a subwavelength metallic waveguide. In this article we highlight the problem of the excitation of a surface plasmon polariton wave on a gold-air interface by a diffraction grating. Our calculations are performed using the Green's function formalism. This formalism allows us to calculate the field diffracted by any structure deposited on the surface of a prism, or a multilayered system, for a wide range of illumination fields (plane wave, dipolar field, focused gaussian beam, ...). In the first part we optimize a finite grating made of simple objects deposited on or engaged in the metal with respect to the geometrical parameters. In order to optimize the performances of this device, we propose to use a pattern of resonant particles studied in the second part, and show that a composite dielectric/metallic particle can resonate in presence of a metallic surface and can be tuned to a specific wavelength window by changing the dielectric part thickness.

**Keywords:** Surface plasmon polariton wave, numerical simulation, diffraction grating, Green's tensor method, resonant nanoparticles

## 1. INTRODUCTION

Surface plasmon polaritons waves (SPPW) are electromagnetic modes confined in the close vicinity of a metal-dielectric interface. They can propagate on several hundred micrometers and can be used in a large variety of domains, from light processing devices to the study of biologically active macromolecules.<sup>1,2</sup> For all these applications, the efficient coupling of a macroscopic external field to the surface mode is a key issue, which still remains quite challenging. Indeed, the wavelength of a SPPW is shorter than the wavelength of the incoming light, and therefore cannot be excited by a full propagating wave as the parallel component of the wavevector of the incident light should be larger than the maximal value permitted in the medium of incidence. In the standard Kreshmann configuration, an evanescent wave created by total internal reflection on an interface with a more refractive dielectric medium allows to fulfill this condition.<sup>3</sup> The most common realization of this geometry is a thin metallic film deposited on a glass substrate, illuminated from the glass in total internal reflection. By conservation of the parallel component of the incoming light wavevector, the SPPW can be fully excited on the opposite vacuum-air interface.<sup>4</sup>

An alternative method is the utilization of a localized object, such as the tip of a surface near-field optics microscope or a defect deposited on the interface, which diffracts an incoming wave in many components both propagating and evanescent: a part of these waves match the excitation condition of the surface plasmon.<sup>5,6</sup> For example, it has been shown by J. Krenn *et al.* that it is possible to use one or several metallic stripes deposited on a gold slab in order to excite the SPPW with a very good efficiency, and then perform a large variety of experiments.<sup>7,8</sup> Additionally, the creation of a SPPW by a diffraction grating could be useful in the technology of long-range surface plasmon (LRSP). Indeed, these waves are supported by symmetric films and

---

Further author information: (Send correspondence to G.L.)

G.L.: E-mail: gaetan.leveque@epfl.ch, Telephone: +41 (0)21 693 47 71

can propagate over several hundreds of micrometers, since no radiative losses occur. On the other hand, the direct excitation of the surface plasmon is not possible.

Any practical realization of a coupling structure is finite, which rises the question of the optimal grating geometry for the best energy transfer between the external field and the surface mode. The corresponding parameter space is very large, and cannot be fully explored by experimental means. In this article, we present a numerical study of the SPPW excitation by finite gratings with a small number of periods. We have performed computation with the Green's dyadic tensor method, based on the resolution of the Lippmann-Schwinger equation of the electric field. It is well-suited for the study of localized object embedded in a dielectric or metallic multilayered medium, both in 2D or 3D geometries.<sup>9-11</sup>

The article is organized as follow: in the first part, we investigate how a finite one-dimensional grating can be optimized to enhance the coupling efficiency between the illumination field and the plasmon. Specifically, we consider the utilization of several localized rectangular stripes deposited on or engraved in a metallic film and study the influence of the periodicity, the height and the width of the pattern for a small number of defects on the coupling efficiency. In the second part, we discuss how the efficiency of these gratings could be improved by using resonant nanoparticles to form the pattern. Moreover, it could be interesting to design tunable objects which resonance can be adapted to a specific experimental setup by varying their geometry, in order to improve the performances of light processing devices, such as band gap structures for filtering or guiding. Then, the spectral response of a gold nanoparticle deposited on a dielectric or metallic substrate is discussed. We will see that a strong displacement of the wavelength peak position occurs if the particle interacts with a metallic substrate: it must therefore be adapted for coupling to a metallic interface. Hence, we propose a particle both composed of dielectric and metallic part, which could be a good candidate in the perspective of designing more efficient surface-plasmon excitation gratings.

## 2. EXCITATION OF A SPPW WITH A METALLIC GRATING

Let us at first consider the characteristics of a SPPW traveling on a free metal-air interface. The dispersion relation of the surface mode is well known<sup>12</sup> and reads:

$$q_{pl} = \frac{\omega}{c} \cdot \sqrt{\frac{\epsilon(\omega)}{\epsilon(\omega) + 1}} \quad (1)$$

where  $q_{pl}$  is the SPPW wavevector,  $\omega$  the angular frequency,  $c$  the speed of light in the vacuum and  $\epsilon(\omega)$  the susceptibility of the metal. For instance, at  $\lambda = 633$  nm, the SPPW wavelength is 596 nm, and its propagation length 12.1  $\mu\text{m}$ . This equation is plotted in Fig. 1(a) for a Drude-like metal susceptibility.

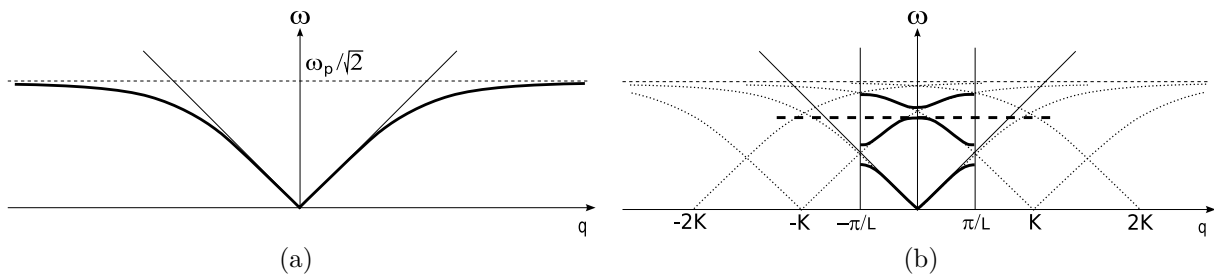


**Figure 1.** (a) Dispersion curve of the SPPW mode propagating at a free metal-air interface. The diagonal solid lines correspond to the light lines  $\omega = |k|c$ . The dispersion curve is under the light lines, then the plasmon mode cannot be excited by a full propagative wave. (b) Bold solid line : plasmon dispersion curve in the first Brillouin zone of the surface plasmon mode propagating at a metal-air interface coupled to a diffraction grating of period  $L$ .

When an infinite unidimensionnal grating of periodicity  $L$  is added onto the interface, the dispersion relation is modified.<sup>13</sup> In a first step, the curve is repeated periodically in the reciprocal space each  $mK = m2\pi/L$ , where  $m$  is an integer and  $K$  the unit Bloch vector of the grating (see Fig. 1(b)). The modes of the system

interface+grating are then described by a wavevector inside the first Brillouin zone  $[-\pi/L, \pi/L]$ . At the crossing points, two modes interact strongly which lifts a degeneracy: a band gap is then formed between an upper and a lower band. A change of the grating shape will modify the gap width and location, and then the position of the lower and upper extrema. As a consequence, the periodicity of the coupling grating for an incident plane wave in normal incidence ( $q = 0$ ) does not correspond to the plasmon wavelength of the free interface. In the configuration of Fig. 1(b), the bold dashed line represents the wavelength of the excitation light, which intersects the second band curve in  $q = 0$ : the SPPW can be excited by a plane wave in normal incidence. We can notice that the periodicity  $L$  is then smaller than the SPPW of the bare interface.

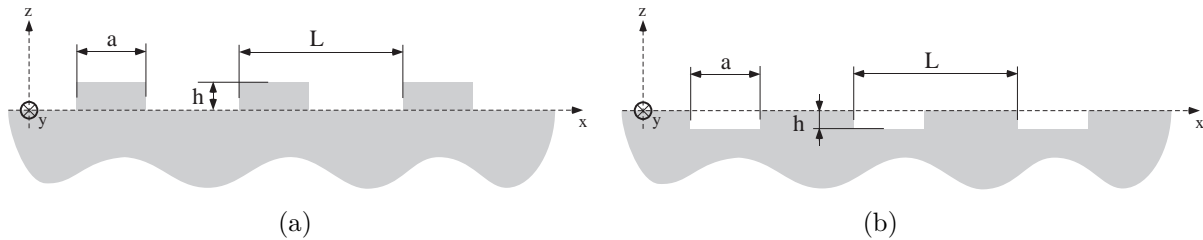


**Figure 2.** (a) Geometrical parameters of a grating of gold rails deposited on a gold half-infinite space. The height of the modulated part is  $h$ , the width of the dots is  $a$ , and its periodicity is  $L$ . (b) In case of a grating of channels,  $a$  is the width of the empty part.

In the following, the unidimensional grating is a set of objects infinitely extended in the  $y$  direction, the interface being overlaid with the  $(Oxy)$  plane. It results into a translation invariance along this  $y$  direction. The upper medium is air, which susceptibility is equal to unity. The metal is gold, which susceptibility is  $\epsilon(\omega)$ . The pattern of the grating has a rectangular cross-section, it is then fully characterized by three parameters (see Fig. 2): the periodicity, labeled  $L$ , the height  $h$  of the modulated part and the width  $a$  of the defect. Additionally, as we are interested in finite gratings, another parameter represents the number of patterns in the structure, which will be set to 5 in order to limit the number of degrees of freedom. Two kind of patterns are studied: when gold is deposited on the interface, we will use the expression *rail*, and when matter is removed from the metal, we will use the expression *channel*.

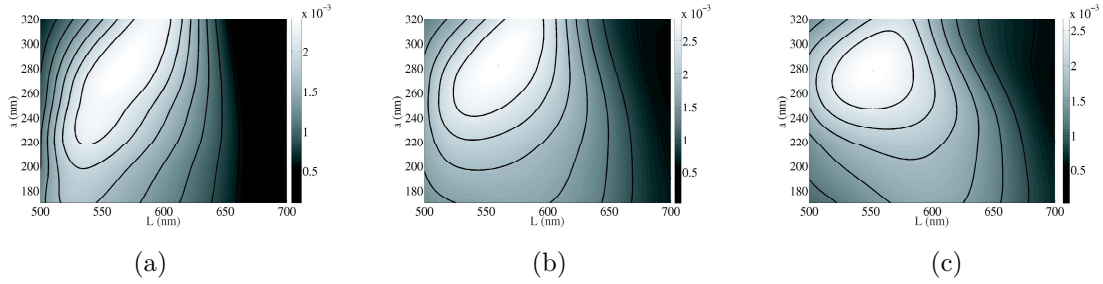
Finally, the grating is illuminated by a monochromatic gaussian beam in normal incidence, which waist  $w_0 = 6 \lambda$  corresponds to the length of the structure. The wavelength is fixed at  $\lambda = 633 \text{ nm}$ .

## 2.1. The half-infinite gold space.

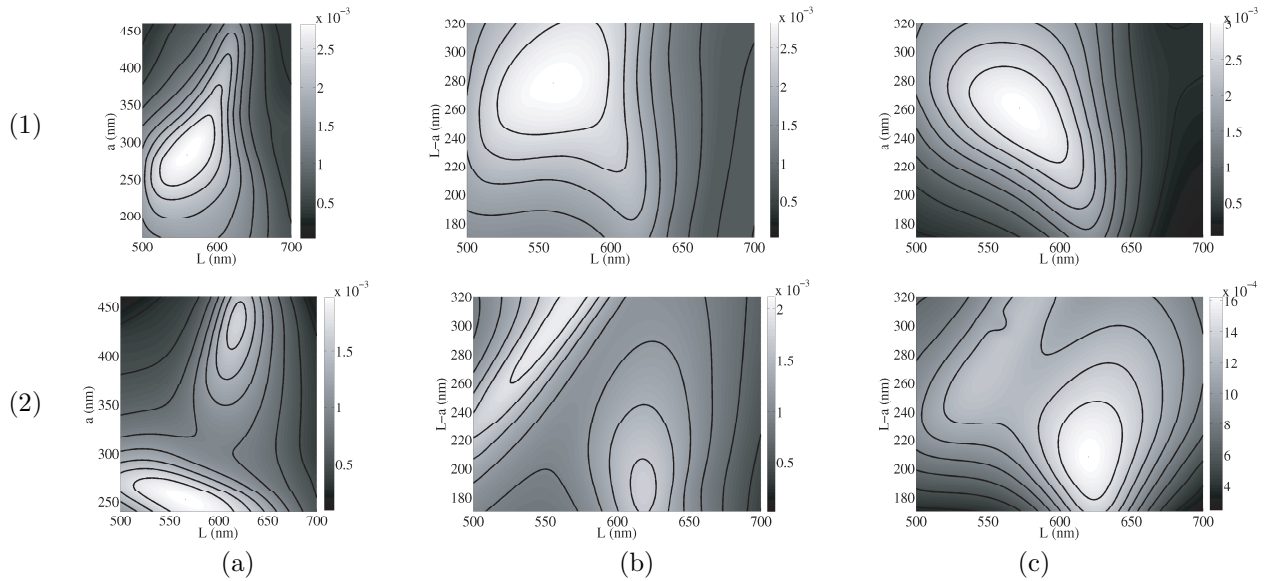
The simplest system is a half-infinite gold space. We have studied excitation of SPPWs by a five patterns grating illuminated in normal incidence, by computing the intensity of the field just above the metallic surface ( $z_0 = 0^+$ ) at  $x_0 = 50 \mu\text{m}$  away from the center of the grating. This field intensity corresponds to that of the SPPWs excited by the grating.

Figure 3 shows the evolution of the grating coupling efficiency as a function of the grating height  $h$ . On each picture is plotted the intensity in  $(x_0, z_0)$  with respect to  $L$  and  $a$ . We can see that the intensity is maximum for a height of 50 nm. The corresponding period and width values are  $L = 550 \text{ nm}$  and  $a = 280 \text{ nm}$ , which correspond to a duty cycle of almost 0.5. Additionally, the fact that  $L < \lambda_{pl}$  shows that the plasmon of the second band is excited (as in Fig. 1).

Figure 4 presents the different results obtained with symmetrical defects, that is an array of channels, as in Fig. 3, and an array of rails. The results should be perfectly identical in the case of an infinite grating excited by a plane wave when the transformation  $L \rightarrow L$ ,  $a \rightarrow L - a$  is applied to the data. This is not strictly the case for a finite grating, because of the relative position of the rails/channels with respect to the flat metal interface. Moreover, this symmetry occurs only in the case of the half-infinite gold space, and disappears with a metallic film of finite thickness: in that last case, the average thickness is increased by a grating of rails and decreased by a grating of channels.



**Figure 3.** Plot of the electric field intensity in  $(x_0 = 50\mu\text{m}, z_0 = 0^+)$ , normalized to the maximal intensity of the incident field, with respect to the periodicity  $L$  and the width of the defect  $a$ , for several height  $h$  of the modulated part: (a)  $h = 40$  nm, (b)  $h = 50$  nm and (c)  $h = 60$  nm.



**Figure 4.** Plot of the intensity in  $(x_0, z_0)$  normalized to the maximal intensity of the incident field, with respect to the periodicity  $L$  and the width of the defect  $a$ . Plots labelled (1) (respectively (2)) are computed for  $h=50$  nm (respectively  $h=80$  nm). Plots labelled (a) (respectively (c)) corresponds to channels (respectively rails) of width  $a$ . For the plots labelled (b), datas are the same as (a) but plotted as a function of  $L$  and  $L - a$ .

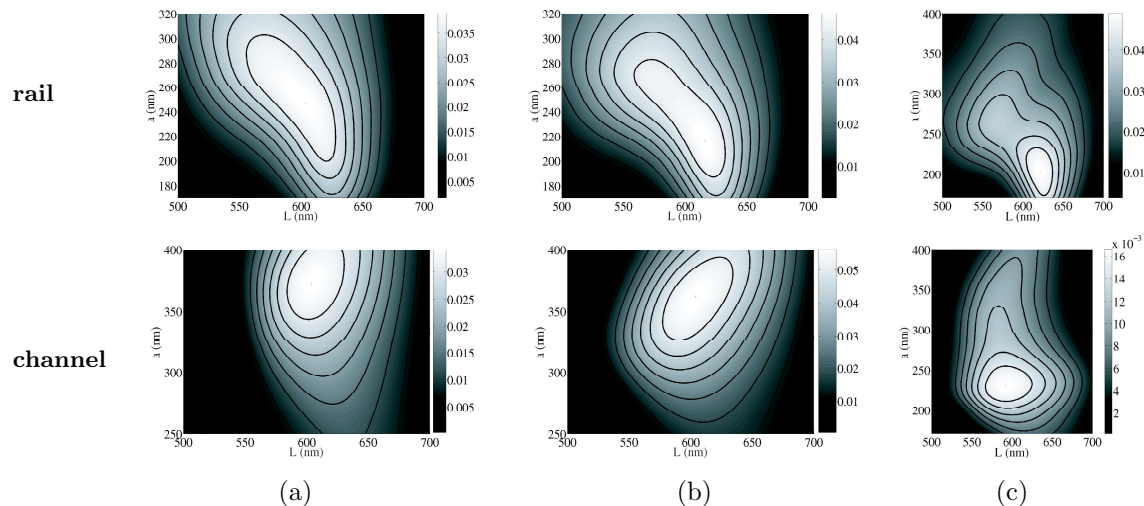
In this figure, the first (respectively second) line shows the results obtained with a 50 nm (respectively 80 nm) thick grating. The first column corresponds to a grating of channels, and the third one corresponds to a grating of rails. The two plots of the second column show the same data as the first one, but the quantity  $L - a$  is reported on the vertical axis. This quantity represents the width of the metallic (respectively air) part in case of channels (respectively rails) grating.

We can first note by comparing column 2 and column 3 of the first line that this symmetry is rather well verified, the amplitudes and the positions of the maxima being quite similar. But for  $h=80$  nm, the comparison is good only qualitatively. Let us note that two maxima appear on these pictures. The one of the largest period is located around  $L = 633$  nm which corresponds to the illumination wavelength: just above this critical value, the first diffraction order which is fully evanescent for  $L < \lambda$  become radiative and diffracts parallel to the interface. Additional simulations have shown that the amplitude of this first diffraction order is very weak compared to the plasmon amplitude up to  $h=50$  nm in the case of rails, and  $h=70$  nm in the case of channels. The fact that the first order seems to appear for lower values of  $L$  than the wavelength is probably due to the finite size of the grating, which increases the number of wavevector supplied by the grating (in other words, the grating

transmittivity is broader-band than it would be for an infinite grating).

## 2.2. The symmetric gold film.

A SPPW localized near the free interface of a thin metallic slab does no longer obey the dispersion relation of Eq. 1. When the thickness of the metallic layer is similar to the penetration depth of the plasmon wave in the metal, the SPPW can feel the other surface and excite the corresponding wave. This coupling between the two interfaces produces two new modes. If the surrounding dielectric material is the same on each side, one is characterized by a symmetric parallel component of the electric field with respect to the middle of the slab, while the other is antisymmetric.<sup>14,15</sup> This last one is the longest range wave. For example, for a symmetric 70 nm thick gold slab at 633 nm in air, the wavelength of the antisymmetric mode is 609 nm, and its range is 31.2  $\mu\text{m}$ . For comparison, the symmetric mode has a wavelength of 580 nm and a range of 5.8  $\mu\text{m}$ .



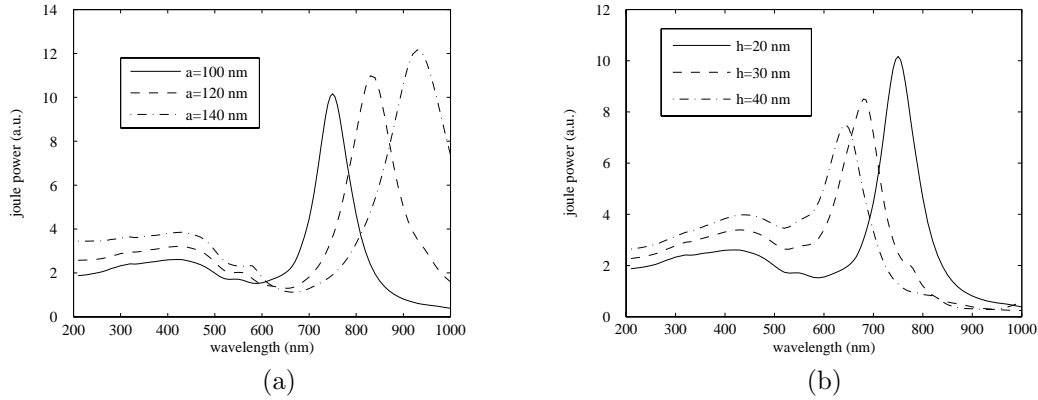
**Figure 5.** First (respectively second) line: plot of the normalized intensity in  $(x_0, z_0)$  of the plasmon diffracted by a rails (respectively channels) grating deposited on a 70 nm thick symmetric gold layer. The surrounding medium is air. The height of the modulated part is varied : (a)  $h = 40$  nm, (b)  $h = 50$  nm and (c)  $h = 60$  nm.

Figure 5 shows the normalized electric field intensity in  $(x_0, z_0)$  with respect to the parameters  $L$  and  $a$  for a five patterns grating deposited on a 70 nm thick gold layer surrounded on both sides by air. The first (respectively second) line shows the results for a rails (respectively channels) pattern. The height of the defects is increased from 40 to 60 nm. In the case of rails, the best efficiency coupling is obtained for  $h = 50$  nm,  $L = 580$  nm and  $a = 270$  nm which gives a duty cycle slightly smaller than 0.5. Additionally, as in Fig. 4, a second maximum appears when  $h$  is larger than 60 nm, which corresponds to the fact that the first diffraction order, which is radiative, is sufficiently intense to dominate the plasmon wave intensity. A comparison between the plots of the first line and those of the second allows us to verify that the rails/channels symmetry does not occur for a finite thickness slab. Indeed, the best duty cycle is about 0.6 for  $h < 60$  nm and 0.4 for a larger thickness. The optimal parameters for the channel configuration are  $h = 50$  nm,  $L = 600$  nm and  $a = 360$  nm, for which the field intensity is larger than the optimized value in rails configuration. Hence a grating of channels seems to be a better way to excite a SPPW than a rails array.

In the two configurations we have discussed in this section, the half-infinite gold space and the symmetric gold slab, the parameters allowing the best coupling efficiency corresponds to a duty cycle of about 0.5-0.6, and a modulation height of 50 nm. It is possible to evaluate the power transferred to the SPPW by computing the norm of the difference between the incident Poynting vector and the transmitted one: the coupling efficiency is about 45%, that is 22% in each direction in the case of the half-infinite gold space, and 33% (16% in each direction) for the symmetric gold slab (under normal incidence as it is the case in this paper, two SPPWs are equally excited, one in the forward direction and one in the backward direction). We can wonder how this number could be

increased. One possibility could be to improve the intensity of the field scattered by one individual particle, for instance by the use of resonant particle. This is the subject of the next part.

### 3. RESONANT NANOPARTICLE ON A METALLIC FILM



**Figure 6.** Evolution of the spectrum of a three-dimensional gold nanoparticle deposited on a dielectric film ( $n=1.5$ ). The horizontal section of the particle is a square of lateral dimension  $a$  and its thickness is  $h$ ; (a) the height is fixed to  $h=20$  nm and the width is increased from 100 to 140 nm; (b) the width is fixed to  $a=100$  nm and height is increased from 20 to 40 nm.

When illuminated by an incident field, the intensity of the light scattered by a metallic nanoparticle presents one or several resonances. This phenomenon has its origin into the excitation of a volume plasmon inside the nanoparticle. The number and amplitude of these resonances depend strongly on the geometrical parameters of the particle (shape, volume) but also on the characteristics of the incoming field (direction, polarization ...) and on the surrounding (for instance the presence of a dielectric or a metallic interface nearby).<sup>16, 17</sup>

As an illustration, Fig. 6(a) shows the joule power, relied to the absorption cross section, dissipated inside a three-dimensional gold nanoparticle deposited on a glass substrate of index  $n=1.5$ . This particle has a square horizontal cross section of lateral dimension  $a$ , and its thickness is  $e_m = 20$  nm. The particle is illuminated under normal incidence through the glass, and the polarization of the electric field is along one of the lateral faces. The width is varied from  $a = 100$  nm to  $a = 140$  nm. For  $a = 100$  nm, the resonance is around 750 nm. When the width is increased, the peak is red-shifted. On the other hand the resonance is *blue*-shifted from 750 nm to 640 nm when the thickness  $e_m$  is increased from 20 nm to 40 nm, as can be seen on Fig. 6(b). Hence particles can be designed in order to fit the resonance with a specific wavelength or frequency window.

This resonant property is strongly affected by the presence of a metallic interface in its vicinity. Figure 7(a) shows the evolution of the particle spectrum when it is located at a distance  $d$  from the metal, representing the empty space between the bottom of the particle and the interface (see Fig. 7(b)). When  $d > 100$  nm, the displacement of the peak is negligible compared to its width. But its position is strongly modified when  $d < 20$  nm. At the limit of contact, the resonance is shifted towards the far infrared. Hence, a nanoparticle of some tens of nanometers size deposited directly on a metallic film does not resonate in the visible range. For specific applications, it could be interesting to keep these particles resonant even in presence of a metallic substrate.

One first possibility is the introduction under the gold particle of a dielectric layer covering the whole gold slab. But it implies that both the properties of the particle and the dispersion relation of the film are modified, which can be a problem in some applications. Then, another solution is to design composite particles made of both a dielectric and a metallic part (see Fig. 8(a)). In this section, we present some results on this particular geometry.

The dielectric part of the particle is  $e_d$  nanometers thick, the metallic part is  $e_m$  nanometers thick, and the lateral size  $a$  of its square cross section is fixed to 100 nm. The particle is illuminated under normal incidence

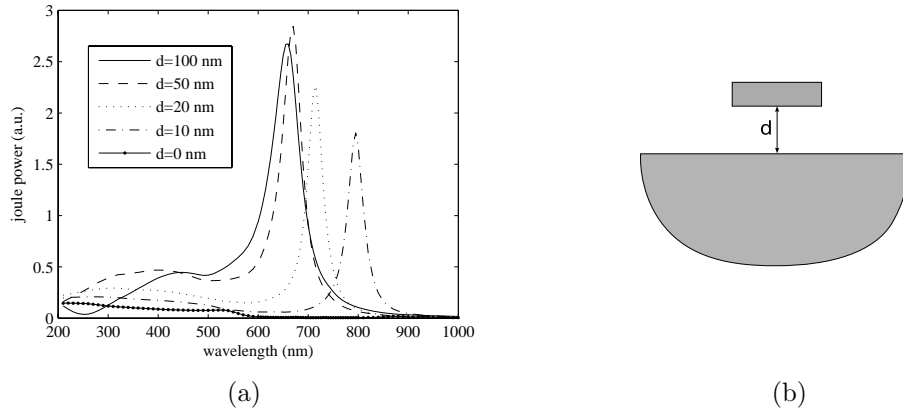


**Figure 7.** Evolution of the spectrum of a gold particle of size  $100 \times 100 \times 20 \text{ nm}^3$  with the distance  $d$  between the bottom of the particle and the gold-air interface.

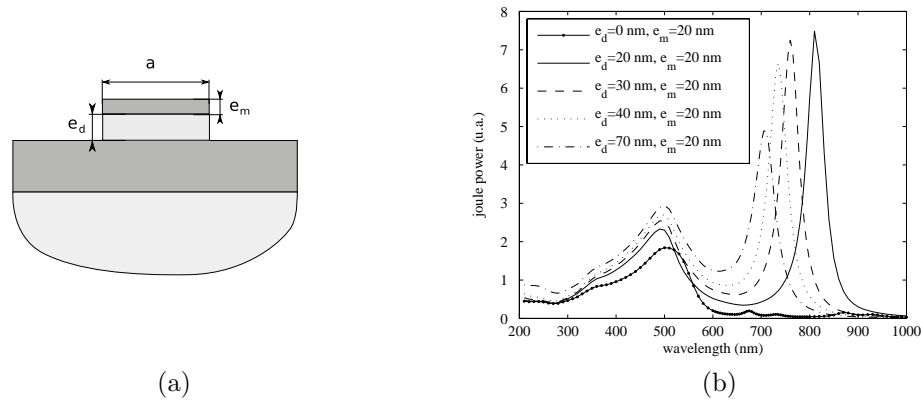


**Figure 8.** (a) Geometry and parameters of the composite three dimensional particle.  $e_d$  (resp.  $e_m$ ) is the thickness of the dielectric (resp. metallic) part. The gold slab is 50 nm thick. (b) Variation of the spectrum of the nanoparticle for several values of the dielectric thickness  $e_d$ . The width  $a$  and the metallic thickness  $e_m$  are respectively fixed to 100 nm and 20 nm.

by a plane wave linearly polarized along one of the lateral sides. Figure 8(b) shows the joule power dissipated in the metallic part of this particle, with respect to the wavelength of the excitation field. It appears that even a thin dielectric layer (30-40 nm) is sufficient to bring the resonance back to the 700-800 nm window. When  $e_d$  is increased, the resonance is blue-shifted. Hence the thickness of the dielectric spacer can allow tuning the particle to a specific wavelength window.

Figure 9 shows in logarithmic scale the normalized intensity of the electric field in the polarization plane, at the resonance wavelength (760 nm) for  $a = 100 \text{ nm}$ ,  $e_d = 30 \text{ nm}$  and  $e_m = 20 \text{ nm}$ . The field appears to be strongly confined between the particle and the metallic surface. The high value of the intensity on the lateral side of the object is due to the discontinuity of the parallel component of the electric field at the edge. It produces an amplification of  $|\epsilon|^2$  from inside to outside the particle. This picture indicates that the field scattered by the particle is strongly coupled to the plasmon mode of the interface, which is an encouraging point for future calculations of gratings of composite particles as light-plasmon couplers.

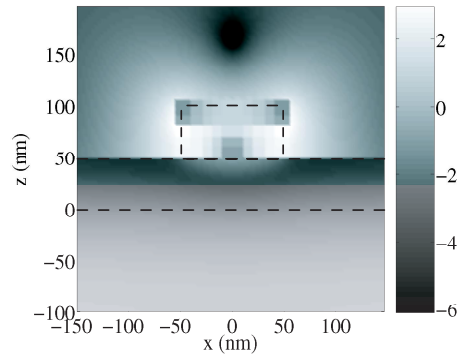


**Figure 9.** Normalized intensity of the electric field in logarithmic scale, plotted in the polarization plane of the incident plane wave.

#### 4. CONCLUSION

We have presented numerical simulations on finite gratings engraved in or deposited on a gold-air interface, by considering at first the case of a half-infinite gold space and then a symmetric gold slab surrounded by air, at the wavelength of  $\lambda = 633$  nm. The geometrical parameters of these gratings have been optimized for a five patterns grating. In both cases, the optimal duty cycle is approximately 0.5, the optimal modulation height is 50 nm, and the best grating periodicity is smaller than the SPPW wavelength. More specifically, we have verified that there is almost no difference in the response between an array of dots and an array of holes in the case of the half-infinite gold space, which corresponds to a rigorous property of the infinite grating illuminated by a plane wave. However, this symmetry is broken for a finite thickness slab: the position of the maxima are then totally different (duty cycle  $\approx 0.6$  for  $h < 60$  nm and  $\approx 0.4$  above), due to the fact that the average thickness of the slab is larger for an array of rails than for an array of channels. In this situation, the grating of channels is the more efficient.

In order to improve the efficiency of the coupling, we suggest to use resonant nanoparticles as grating element. A promising candidate is a composite particle made of both dielectric and metallic part, the first one playing the role of spacer between the metallic slab and the gold dot. The main result is that the position of the resonance wavelength can be tuned by changing the thickness of the dielectric part. A particle resonant at 750 nm when deposited on a glass substrate can be kept resonant around this wavelength in the presence of a 50 nm thick gold slab by using a dielectric spacer with thickness of only 30 nm to 40 nm.

#### ACKNOWLEDGMENTS

The authors thank J. C. Weeber from Laboratoire de Physique de l'Université de Bourgogne for fruitful discussions. Partial funding from the FP6 IST Network of Excellence Plasco-Nano-Devices from the European Commission is gratefully acknowledged.

#### REFERENCES

1. J. Ditinger, S. Klein, F. Bustos, W. L. Barnes, and T. W. Ebbesen, "Strong coupling between surface plasmon-polaritons and organic molecules in subwavelength hole arrays," *Phys. Rev. B* **71**, p. 035424(5), 2005.
2. F. Yu and W. Knoll, "Immunosensor with self-referencing based on surface plasmon diffraction," *Anal. Chem.* **76**, pp. 1971–1975, 2004.
3. A. Otto, "Excitation of nonradiative surface plasma waves in silver by the method of frustrated total reflection," *Z. Phys.* **216**, pp. 398–410, 1968.
4. F. I. Baida, D. V. Labeke, and J. M. Vigoureux, "Theoretical study of near-field surface plasmon excitation, propagation and diffraction," *Optics Commun.* **171**, pp. 317–331, 1999.



5. S. I. Bozhevolnyi, V. S. Volkhov, A. Boltasseva, and K. Leosson, "Local excitation of surface plasmon polaritons in random surface nanostructures," *Optics Commun.* **223**, pp. 25–29, 2003.
6. A. V. Zayats, I. Smolyaninov, and A. A. Maradudin, "Nano-optics of surface plasmon polaritons," *Phys. Rep.* **408**, pp. 131–314, 2005.
7. H. Ditlbacher, J. R. Krenn, G. Schider, A. Leitner, and F. R. Aussenegg, "Two-dimensional optics with surface plasmon polaritons," *Appl. Phys. Lett.* **81**, p. 1762(3), 2002.
8. H. Ditlbacher, J. R. Krenn, A. Hohenau, A. Leitner, and F. R. Aussenegg, "Efficiency of local light-plasmon coupling," *Appl. Phys. Lett.* **83**, p. 3665(3), 2003.
9. O. J. F. Martin and N. B. Piller, "Electromagnetic scattering in polarizable backgrounds," *Phys. Rev. E* **58**, p. 3909(7), 1998.
10. M. Paulus, P. Gay-Balmaz, and O. J. F. Martin, "Accurate and efficient computation of the green's tensor for stratified media," *Phys. Rev. E* **62**, p. 5797(11), 2000.
11. G. Lévêque, R. Mathevet, J. Weiner, G. C. des Francs, C. Girard, R. Quidant, J. C. Weeber, and A. Dereux, "Modelling resonant coupling between microring resonators addressed by optical evanescent waves," *Nanotechnology* **15**, pp. 1200–1210, 2004.
12. *Introduction to surface and superlattice excitations*, Cambridge University Press, New York, 1989.
13. W. L. Barnes, T. W. Preist, S. C. Kitson, and J. R. Sambles, "Physical origin of photonic energy gaps in the propagation of surface plasmons on gratings," *Phys. Rev. B* **54**, p. 6227(18), 1996.
14. D. Sarid, "Long-range surface-plasma waves on very thin metal films," *Phys. Rev. Lett.* **47**, pp. 1927–1930, 1981.
15. J. Burke and G. I. Stegeman, "Surface-polariton-like waves guided by thin, lossy metal films," *Phys. Rev. B* **33**, p. 5186, 1986.
16. J. P. Kottmann, O. J. F. Martin, D. R. Smith, and S. Schultz, "Non-regularly shaped plasmon resonant nanoparticle as localized light source for near-field microscopy," *J. Microsc.* **202**, pp. 60–65, 2001.
17. J. P. Kottmann, O. J. F. Martin, D. R. Smith, and S. Schultz, "Plasmon resonances of silver nanowires with a nonregular cross section," *Phys. Rev. B* **64**, p. 235402, 2001.